Macromolecules

ARTICLE

pubs.acs.org/Macromolecules

Ring Walking versus Trapping of Nickel(0) during Kumada Catalyst Transfer Polycondensation Using Externally Initiated Electron-Accepting Thiophene−Benzothiadiazole−Thiophene Precursors

H. Komber,[†] V. Senkovskyy,[†] R. Tkachov,[†] K. Johnson,[‡] A. Kiriy,[†] W. T. S. Huck,[§,∥] and M. Sommer*[,§]

[†]Leibniz-Institut für Polymerforschung Dresden e.V., Hohe Strasse 6, 01069 Dresden, Germany

[‡]Cavendish Laboratory, J J Thomson Avenue, Cambridge CB3 0HE, U.K.

[§]Melville Laboratory for Polymer Synthesis, Lensfield Road, Cambridge CB2 1EW, U.K.

[∥]Radboud University Nijmegen, Heyendaalseweg 135, 6525 AJ Nijmegen, Netherlands

Supporting Information

ABSTRACT: Interactions of Ni(0) and thiophene−benzothiadiazole−thiophene (TBT) units during the Kumada catalyst transfer polycondensation (KCTP) of 2-chloromagnesio-5-bromo-3-hexylthiophene (**1**) are investigated. Monofunctional TBT initiator precursors are used for the external initiation of KCTP, and the mechanism of initiator activation and polymerization is elucidated using NMR and MALDI-ToF MS. We find that the activation of the TBT-bromide initiator precursor using nickel−diethylbipyridine ($NiEt_2bipy$) occurs via a two-step pathway, in which $NiEt_2bipy$ coordinates to benzothiadiazole (B) first, followed by the elimination of butane and oxidative addition of liberated Ni(0)bipy into the terminal TBT−Br bond. It is shown that the B unit traps Ni(0) during the KCTP of **1**, which results in significant termination, as derived from the degree of bromine-terminated chains. The ability of B units to trap Ni(0) is further illustrated by using a symmetric bifunctional Br-TBT-Br initiator precursor for the KCTP of **1**, during which Ni(0) is not able to "ring walk" over the B unit to initiate polymerization at the other end of the chain. These results are important for the design of well-defined and electronically end-functionalized conjugated polymers, but also for understanding termination mechanisms in KCTP in general.

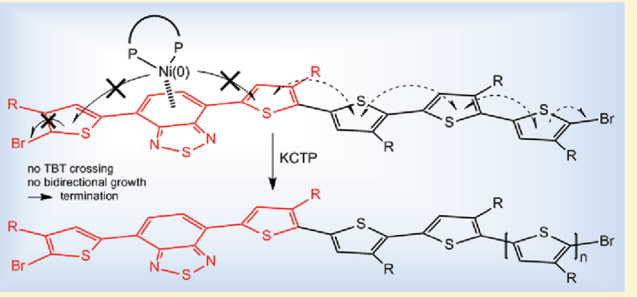

INTRODUCTION

Conjugated polymers (CPs) show great promise as active materials for cheap, printable, large-area, lightweight, and flexible polymeric organic devices.[1] The great chemical versatility in the design of monomer building blocks has led to numerous CPs with tailorable properties for the use in organic field-effect transistors,[2] solar cells,[3] sensors,[4] lasers,[5] and light-emitting diodes.[6] Classical step-growth polycondensations such as Suzuki,[7] Stille,[8] or Sonogashira[9] couplings are widely used to synthesize CPs. Chain-growth polymerizations are less developed and are restricted to a limited range of monomers. Several methods are notable here, including ring-opening metathesis polymerization,[10,11] Suzuki chain-growth polycondensation,[12] nitroxide-mediated polymerization,[13] and nickel-catalyzed chain-growth Kumada catalyst transfer polycondensation (KCTP).[14−16] The latter polymerization follows an intriguing "ring-walking" mechanism that imparts a living character to the reaction. The controlled character of KCTP therefore offers important advantages over traditional step-growth methods, such as predetermined molecular weight and low polydispersities. Moreover, more advanced, multifunctional polymer architectures such as all-conjugated block copolymers are potentially easily accessible via one-pot reactions, which are otherwise difficult or circuitous to prepare. The conventional initiation of KCTP makes use of commercially available catalysts such as $Ni(dppp)Cl_2$, which generates an initiating dimer from two monomer molecules.[14−16] Thus, end group modification is only possible via quenching the polymerization with Grignard compounds[17−20] or by using postpolymerization reactions.[21,22] The external initiation of KCTP via functional nickel initiators provides an elegant tool to graft conjugated polymers from an initiator that carries functional groups. Thus, conjugated polymers can be functionalized in high yield.[14] Up to now, surface-initiated polymerization[23] and substrates such as phenyl- or tolyl-based silyls[24] and phosphonates,[25] silica particles,[26] polystyrene,[27] hexaphenylbenzene,[28] or alkoxyamines[29] have been used for the external initiation of KCTP in order to create different polymer topologies or incorporate reactive groups for postpolymerization reactions.

Received: August 17, 2011
Revised: October 21, 2011
Published: November 15, 2011

While without doubt conceptually promising, the external initiation of KCTP requires further exploration into different directions in order to assess its full potential. For instance, the ability to decorate conjugated polymers with any functional π-system will enable the preparation of conjugated materials with precisely positioned functions in which energy or electrons can be cascaded along the polymer chain toward desired directions. Considering that during KCTP Ni(0) is delocalized over the conjugated polymer between each reductive elimination and oxidative addition step, backbones incorporating different aromatic initiator moieties will display different affinities toward Ni(0). The knowledge of such behavior is of fundamental interest since it will determine the degree of control during polymerization. Very recently, we have demonstrated a convenient approach to externally initiate the KCTP of 2-chloromagnesio-3-hexyl-5-bromothiophene **1** using sterically hindered Grignard compounds and have successfully initiated 4-(5-(9,9-dioctylfluorene)-4-hexyl-2-thienyl)-7-(5-bromo-4-hexyl-2-thienyl)-2,1,3-benzothiadiazole (F8TBT-Br).[30]

The thiophene−benzothiadiazole−thiophene (TBT) motif is often used as a building block with other comonomers in small band gap conjugated polymers.[3] For example, TBT copolymers with fluorene show ambipolar transport behavior in field-effect transistors[31] and can be used either as p-type[32] or n-type[33] material. In addition, the strong red photoluminescence of conjugated polymers containing TBT units has made such materials interesting candidates for light-emitting devices.[34] The investigation of the interaction of Ni(0) with TBT and other electron-deficient aromatic groups during polymerization will also aid in the development of new monomers for KCTP.

Here, we use nickel−diethylbipyridine ($NiEt_2$bipy **2b**) ("the Nibipy route")[26] to activate monofunctional F8TBT-Br (**2a**) and bifunctional Br-TBT-Br (**5**) and convert them into initiators for the KCTP of 2-chloromagnesio-3-hexyl-5-bromothiophene (**1**). We show that interactions of nickel with B lead to a drastically altered polymerization behavior of the otherwise robust KCTP method. The origin of resulting side reactions is analyzed in detail, and ways to overcome them are discussed.

EXPERIMENTAL SECTION

Materials. 4-(5-(9,9-Dioctylfluorene)-4-hexyl-2-thienyl)-7-(5-bromo-4-hexyl-2-thienyl)-2,1,3-benzothiadiazole (**2a**, F8TBT-Br),[30] 4,7-bis(5-bromo-4-hexyl-2-thienyl)-2,1,3-benzothiadiazole (**5**, Br-TBT-Br),[34] 2-chloromagnesio-3-hexyl-5-bromothiophene (**1**),[35] and $NiEt_2$bipy (**2b**)[36] were synthesized as described elsewhere. Dppe was purchased from Aldrich and used as received. THF and deuterated THF were purchased in anhydrous grade and further distilled over sodium benzophenone ketyl.

Synthesis. *General Procedure of External Initiation (Preparative Scale).* In a glovebox, 190 mg (0.203 mmol) of **2a**, 55 mg (0.20 mmol) of $NiEt_2$bipy **2b**, and 89 mg (0.22 mmol) of dppe were dissolved in 3, 2, and 2 mL of THF, respectively, and the solutions were back-transferred outside the glovebox via syringe. In case of Br-TBT-Br **5**, 0.5 equiv of $NiEt_2$bipy was used. A 100 mL single-necked flask equipped with a magnetic stirrer and a septum was flame-dried under vacuum, cooled down, and backfilled with argon. The F8TBT-Br solution was injected and stirred at room temperature. $NiEt_2$bipy was added slowly via syringe, and the completion of reaction was spotted by a characteristic color change from the immediately appearing brown color to deep purple. The dppe solution was then added via syringe, and the solution was stirred for 1 min. To start polymerization, a solution of **1** (4 mmol) in 40 mL of THF was added, and the whole was stirred for 20 min. Kinetic samples were taken via syringe, quenched with hydrochloric acid, precipitated into methanol, analyzed via GPC and MALDI-ToF, and then further extracted with methanol and warm hexanes. After extraction with hexanes, samples were subjected to GPC, MALDI-ToF, and NMR analysis again. The residual polymerization mixture was quenched by adding hydrochloric acid (1 M in methanol), stirred for 5 min, and then further precipitated by adding methanol. Filtration into a Soxhlet thimble was followed by extraction with methanol, hexanes, and chloroform, and the chloroform fraction was passed through a plug of silica gel. The chloroform was removed under reduced pressure, methanol was added, and the solids were collected via filtration and dried at 40 °C overnight.

Typical Procedure of External Initiation (in Situ NMR Experiment). In a glovebox, 10 mg (0.01 mmol) of **2a**, 3 mg (0.01 mmol) of $NiEt_2$bipy **2b**, and 4 mg (0.01 mmol) of dppe were dissolved in 0.5, 0.1, and 0.1 mL of deuterated THF, respectively. A NMR tube was filled with the F8TBT-Br solution and closed with a septum. After acquiring the desired spectra at 0 °C, the $NiEt_2$bipy solution was injected and the tube was shaken. Cooling to −20 °C gave enough time to acquire all spectra of the precomplexation stage. The sample was allowed to warm to 10 °C, which promoted oxidative addition and the release of butane, as could be followed by ^{1}H NMR. Spectra of the formed complex were measured at 0 °C. The dppe solution was added via syringe at 0 °C. This NMR tube solution was finally used to initiate KCTP of **1**. The solution was transferred back to a syringe and quickly added to a solution of 0.32 mmol of **1** in 3.2 mL of THF. Workup and purification were carried out as for the preparative scale experiment.

Instrumentation. ^{1}H (500.13 MHz), ^{13}C (125.77 MHz), and ^{31}P (202.46 MHz) NMR spectra were recorded on a Bruker Avance III spectrometer using a 5 mm ^{1}H/^{13}C/^{19}F/^{31}P gradient probe. The ^{1}H spectra of P3HT were recorded at 303 K (unless otherwise noted) using $CDCl_3$ as solvent and were referenced to the residual solvent peak (7.26 ppm). The ^{13}C and ^{31}P NMR spectra were recorded using THF-d_8 as solvent.

GPC measurements were carried out on two PL gel 5 μm mixed C columns, with pore sizes ranging from 10 to 105 Å (Polymer Laboratories), connected in series with a SPD-M20A prominence diode array detector (Shimadzu) and a differential refractometer/viscometer model 200 (Viscotek). Calibration was done using polystyrene standards, THF was used as eluent, and the flow rate was 1.0 mL/min.

MALDI-ToF mass spectra were recorded on an Applied Biosystems 4700 Proteomics Analyzer. Solutions of the analyte were prepared in THF (10^{-4}−10^{-5} M), and dithranol was used as the matrix (0.1 M in THF). Equal amounts of both solutions were mixed and spotted onto the MALDI plate.

UV/vis Data and PL Measurements. UV/vis spectra were recorded on a Hewlett-Packard 8453 spectrophotometer. PL measurements were carried out on a SpectraPro2500i from Princeton Instruments combined with a CCD camera (PIXIS 100-F, Princeton Instruments). The excitation source was a pulsed 470 nm, 80 ps full width at half-maximum, 10 MHz diode laser (PicoQuant LDH400). Films were measured under vacuum (10^{-5} mbar). Solutions were 50 μg/mL in anhydrous THF and measured in quartz cuvettes. Films were spun from 20 mg/mL $CHCl_3$ solutions at 1500 rpm for 60 s onto Spectrosil quartz substrates. Annealing was done at 200 °C for 10 min followed by cooling at 10 K/min. All preparations were done in a N_2 atmosphere.

Differential Scanning Calorimetry. DSC was carried out on a DSC Q2000 from TA Instruments. The heating rate was 10 K/min under nitrogen. Curves were taken from the second cycle.

RESULTS AND DISCUSSION

Mechanism of Initiation. We use the "Ni-bipy route"[26] to activate the precursor F8TBT-Br **2a**. The recently reported method of convenient initiation[30] is also applicable here; however, the "Ni-bipy route" is preferable in order to study Ni−TBT

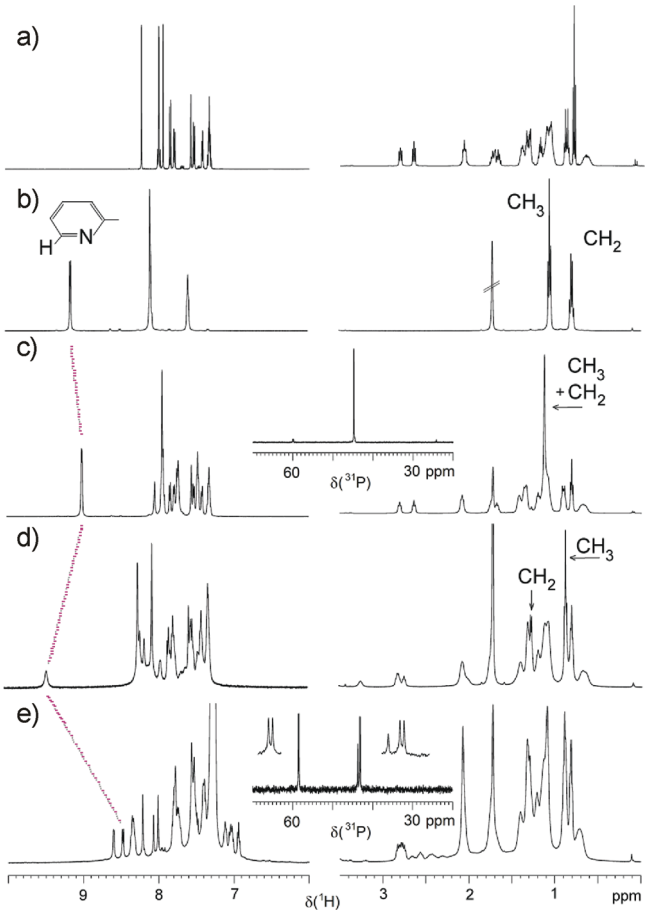

Figure 1. ^{1}H NMR spectra of (a) F8TBT-Br (**2a**), (b) $NiEt_2$bipy (**2b**), (c) precomplex F8TBT-Br/$NiEt_2$bipy **2c** formed from a 1:1 molar mixture of **2a** and **2b** at 0 °C (inset: ^{31}P NMR spectrum of $Ni(dppe)_2$ formed after the addition of dppe to **2c**), (d) F8TBT-Ni(II)bipy-Br **2d** after the reductive elimination of butane and oxidative addition of Ni(0) at 10 °C, and (e) F8TBT-Ni(II)dppe-Br initiator formed after ligand exchange (inset: ^{31}P NMR). All spectra were recorded in THF-d_8 at 0 °C unless otherwise noted. The changes in chemical shifts of the bipy proton and the ethyl groups of $NiEt_2$bipy are indicated. In (d) and (e) free butane is observed and in (e) free bipy.

interactions during initiator synthesis. F8TBT-Br **2a** (Figure 1a) was mixed with $NiEt_2$bipy **2b** (Figure 1b) in dry THF at 0 °C (Scheme 1). An immediate color change from red to brown was observed, accompanied by changes in the ^{1}H NMR spectra of both starting materials (Figure 1c). For F8TBT-Br a shift of the aromatic benzothiadiazole (B) and the neighboring thiophene proton signals occurred, whereas the signal positions of the fluorene unit remained unchanged. Model reactions of $NiEt_2$bipy with either fluorene or TBT confirmed a selective Ni(0)−B interaction. While a mixture of $NiEt_2$bipy and fluorene gave a superposition of the two individual spectra, the two B protons shifted similarly under the presence of $NiEt_2$bipy. A detailed description of the changes in the chemical shifts of the fluorene and TBT protons is given in the Supporting Information (Figures SI-1 and SI-2). Importantly, the proton signals of the bipy ligand of **2c** were different from $NiEt_2$bipy and free bipy. However, the most obvious indication of an interaction between the B moiety and $NiEt_2$bipy is the low-field shift of the CH_2 and CH_3 signals of $Ni(Et)_2$, resulting in an apparent singlet at 1.12 ppm. This singlet is in fact a composite peak of the CH_3 and CH_2 resonances of the ethyl residues of $NiEt_2$bipy/F8TBT-Br **2c**, as evidenced by HSQC and DEPT spectra (see Figure SI-4). Typically, for Ni−Et the ^{13}C chemical shift of CH_2 is lower than that of CH_3 (13.5 vs 16.2 ppm). Further corroboration for the selective B−Ni(0) interaction can be found in the ^{1}H chemical shifts of the α-CH_2 signals of the hexyl side groups, both of which remain unchanged (compare Figures 1a and 1c). The structure of **2c** is very likely but cannot be unequivocally proven from the data available. Attempts to crystallize and isolate complexes of $NiEt_2$bipy and F8TBT-Br were not successful. The addition of dppe at this stage resulted in the formation of $Ni(dppe)_2$, the starting material F8TBT-Br, and free bipy, as evidenced by ^{1}H and ^{31}P NMR (see inset of Figure 1c). When the mixture was warmed up to 10 °C in the absence of dppe, new features appeared in the ^{1}H NMR spectrum (see Figure SI-3), and finally a new spectrum was obtained (Figure 1d). Concomitant with these changes, the color of the reaction mixture turned deep purple. Most significantly, the signal of the bipy ligand shifted, and the formation of butane occurred as confirmed by ^{13}C NMR (see Figure SI-5). Although we cannot assign all signals in this spectrum, obviously a new compound was formed. We ascribe these changes to the formation of complex **2d** (Figure 1d). In addition, slight signal broadening was observed. Since this was more prevalent at higher temperatures, it most likely resulted from exchange processes rather than from the formation of a paramagnetic species. The ligand exchange with dppe was successful at this stage, and the two doublets that are typical for an asymmetric coordination sphere[30] were observed in the ^{31}P spectrum at about 43 and 58 ppm (Figure 1e). The additional singlet at ∼44 ppm arises from the formation of KCTP-inert $Ni(dppe)_2$.[37] We therefore propose that the reaction of $NiEt_2$bipy and F8TBT-Br occurs via precomplexation of $NiEt_2$bipy, in a similar fashion to observations by Yamamoto et al.[38] The resulting complex **2c** is easily destroyed by the addition of dppe, which gives $Ni(dppe)_2$, free bipy, and **2a**. The second step involves reductive elimination of butane and oxidative addition of Ni(0)bipy into the thiophene−bromine bond leading to F8TBT-Nibipy-Br **2d**, which can be finally transformed into the corresponding complex **2e** via ligand exchange (Scheme 1).[26,29,30]

Mechanism of F8TBT-Nidppe-Br Initiated KCTP and Termination. Thus, prepared F8TBT-Nidppe-Br initiators **2e** were used to start KCTP of 2-chloromagnesio-5-bromo-3-hexylthiophene (**1**). For that purpose, **2e** was synthesized in single flasks, and different amounts of **1** were added to vary the chain length. The MALDI-ToF mass spectrum of F8TBT-P3HT **3** with a degree of polymerization of 18 and a PDI of 1.10 is shown in Figure 2b. Clearly, three different species are present, namely the main product F8TBT-P3HT-H, a smaller peak series corresponding to F8TBT-P3HT-Br, and a minor peak series with H/Br-terminated P3HT. A peak series with very low intensity corresponding to Br/Br-terminated P3HT is seen as well. Interestingly, the intensities of the different peak series vary individually throughout the spectrum (the same low molecular weight cutoff for the different peak series is caused by Soxhlet extraction with *n*-hexanes). The corresponding ^{1}H NMR spectrum with complete assignments is shown in Figure 2a. All end groups seen in the MALDI spectrum are observed here as well, and the overall content of F8TBT functionalization (F8TBT-P3HT-Br chains and F8TBT-P3HT-H chains) is calculated to be 77%.

The observation of the different peak series having different molecular weights points to the occurrence of side reactions. We found an acceptable degree of F8TBT functionalization of ∼77% in this sample; however, lower values down to ∼15% were found

Scheme 1. Mechanism of F8TBT-Br Activation Using $NiEt_2bipy$ Followed by Ligand Exchange with Bis-(diphenylphosphinoethane) (dppe)

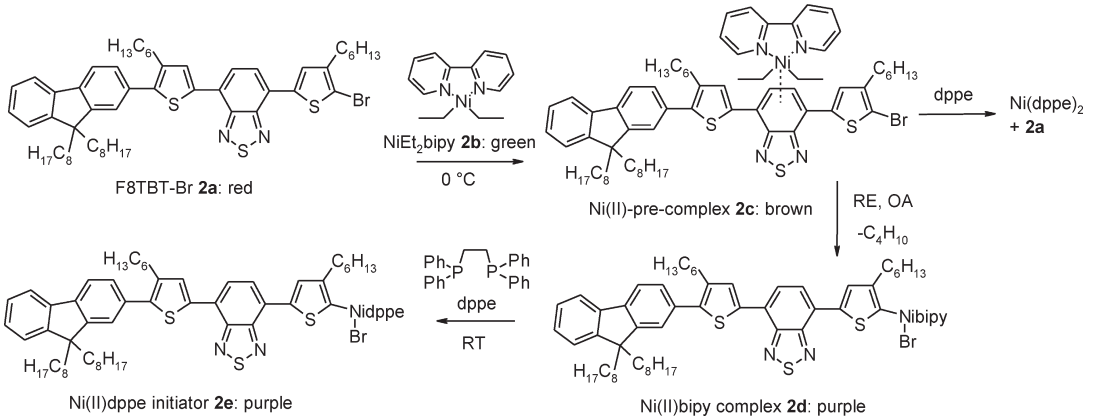

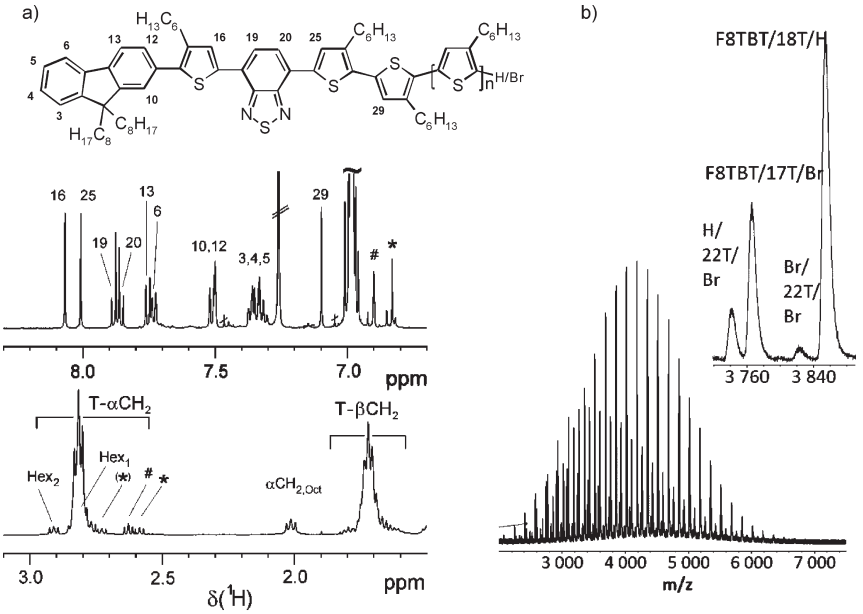

Figure 2. (a) ^{1}H NMR spectrum (regions; $CDCl_3$, 50 °C) of F8TBT-P3HT **3** with assignments (#, signal of the H-terminal groups; ∗, signal of the Br-terminal groups; and (∗), signal of the thiophene unit adjacent to the Br-terminal group). (b) MALDI ToF spectrum of F8TBT-P3HT. The inset shows the enlarged region at around 3800 g/mol, where the four different peak series are assigned.

with increasing monomer-to-initiator ratio. In order to investigate the origin of the reduction in the content of F8TBT-functionalized chains with increasing chain length, we performed kinetic experiments during the F8TBT-Nidppe-Br initiated KCTP of **1** and analyzed the aliquots by GPC and MALDI ToF (Figure 3).

The MALDI spectra of the aliquots qualitatively exhibit the same peaks as already outlined in Figure 2a, namely F8TBT-P3HT-H, F8TBT-P3HT-Br, and H-P3HT-Br terminated chains. The sample taken after 1 min clearly shows that the major peak series arises from the targeted product F8TBT-P3HT-H, which shifts to higher molecular weights with time. Further, a single intense peak with a mass of 1712.72 g/mol is observed in all samples (Figure 3a). This peak is ascribed to the dimer F8TBT-TBTF8 **4** (calculated mass 1712.77 g/mol). **4** is not observed in Figure 2a since that sample was Soxhlet extracted with hexanes, which dissolves the dimer easily. We propose that the reductive coupling of the initiator **2e** causes dimer formation.[24] With this knowledge, the interpretation of the H-P3HT-Br peak series becomes evident. Since reductive coupling of F8TBT-Ni-dppe-Br **2e** not only causes dimer formation but also is expected to produce $NidppeBr_2$,[24,39] we can understand the formation of H-P3HT-Br chains as a result from the conventional initiation of **1** via $NidppeBr_2$ (Scheme 2). We assume that the origin of the coupling reaction lies in the stoichiometry of F8TBT-Br and $NiEt_2bipy$. Yamamoto and co-workers have reported that a solution of Ph-Ni-bipy-Br disproportionates in polar solvents to give biphenyl, while this solution is stable when additional bromobenzene is present.[40] The latter case corresponds to an excess of bromine groups with respect to $NiEt_2bipy$. However, we used 0.95 equiv of $NiEt_2bipy$ to activate **2a**. Using a considerable substoichiometric amount of $NiEt_2bipy$ with respect to the precursor F8TBT-Br is expected to eliminate the coupling reaction and thus conventional initiation of **1**. However,

dx.doi.org/10.1021/ma2018827 |*Macromolecules* 2011, 44, 9164–9172

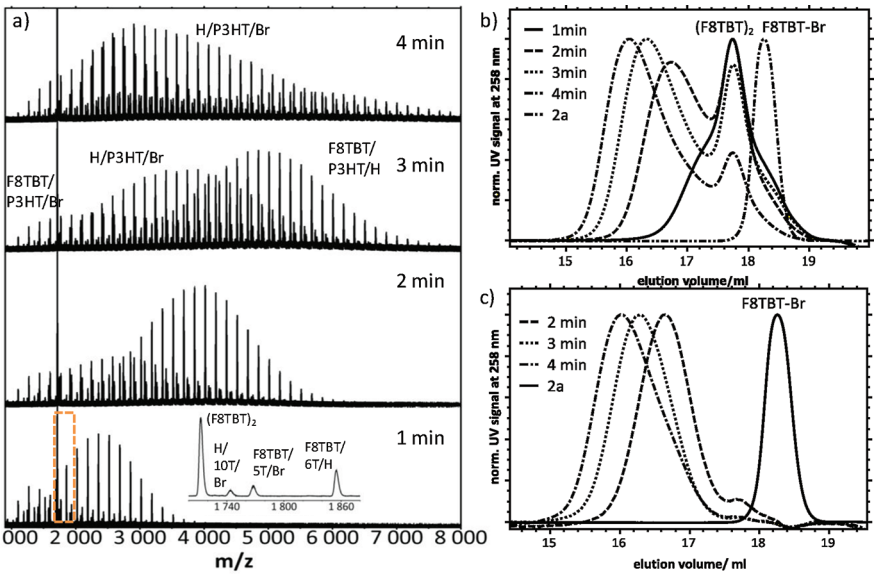

Figure 3. Evolution of molecular weight and end groups during the first minutes in the F8TBT-Nidppe-Br initiated polymerization of **1** via MALDI-ToF and GPC analysis. (a) MALDI-ToF. The inset of the sample taken at 1 min magnifies the region around 1800 g/mol where the dimer **4** and all other species are seen. The corresponding GPC traces are shown in (b) after precipitation in MeOH and in (c) after extraction with warm *n*-hexanes.

Scheme 2. Mechanism of F8TBT-Nidppe-Br Initiated Polymerization of 2-Chloromagnesio-5-bromo-3-hexylthiophene (1) and Termination Reactions[a]

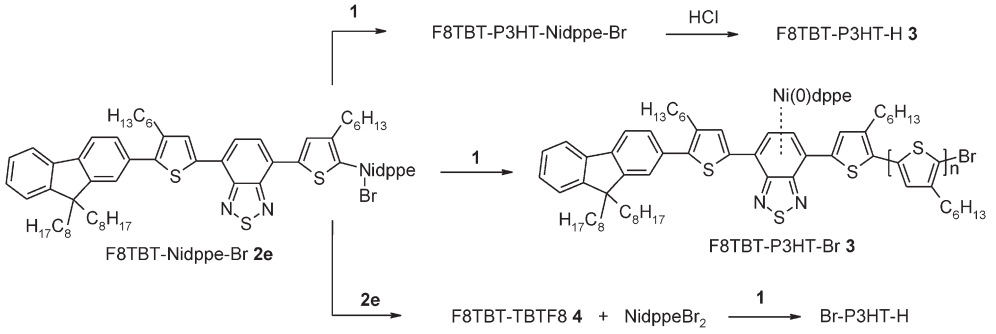

[a] Top: the desired controlled polymerization leads to F8TBT-P3HT-H after quenching with hydrochloric acid. Middle: termination of polymerization occurs when Ni(0) is trapped on the B unit, resulting in F8TBT-P3HT-Br. Bottom: reductive coupling of two molecules of **2e** leads to the dimer **4** and $NidppeBr_2$, which causes conventional initiation of **1**.

decreasing the equivalents of $NiEt_2$bipy to very low values decreases the yield of the initiation reaction as well. One strategy to maximize the content of electronically end-functionalized chains is therefore to precisely balance the amounts of the precursor bromide and $NiEt_2$bipy such that reductive coupling is minimized while the yield of active initiator is maximized. The formation of the dimer **4** is also supported by GPC analysis, which shows a well-defined peak comparable to monodisperse compounds other than the F8TBT-Br precursor (Figure 3b). The dimer and other low molecular weight species can be removed by extracting the samples with *n*-hexanes (Figure 3c). The GPC traces shift to lower elution volumes with increasing polymerization time, in accordance with Figure 3a. The corresponding molecular weights and polydispersities are given in Figure SI-9. We note that although the GPC curves in Figure 3b look acceptably well-defined after extraction with hexanes, these are composite peaks of the species F8TBT-P3HT-Br, F8TBT-P3HT-H, and Br-P3HT-H. Therefore, MALDI-ToF is more informative and will be used for further discussions.

P3HT homopolymer chains with two bromine caps usually indicate termination.[14,39,41] Therefore, F8TBT-P3HT-Br chains are most likely a result of termination. Note that the intensity of the MALDI-ToF signals corresponding to F8TBT-P3HT-Br chains becomes unusually high when compared to $NidpppCl_2$ initiated P3HT chains. (In that case one would look out for Br-P3HT-Br terminated chains, the intensities of which are usually low.[35,41]) This effect is most prevalent for later polymerization times. We also note that termination leads to F8TBT-P3HT-Br from the very beginning of the polymerization, as is seen by the rather unchanged low molecular weight onset of F8TBT-P3HT-Br chains with time. The high molecular weight onset of the F8TBT-P3HT-Br peak series in MALDI, however, extends to higher molecular weight with increasing polymerization time, since growing chains F8TBT-P3HT-Nidppe-Br are continuously converted into terminated species F8TBT-P3HT-Br (Figure 3a). The results from Figure 3 can be summarized as follows: The controlled KCTP of **1** using F8TBT-Nidppe-Br **2e** as an external initiator leads to the desired product F8TBT-P3HT-H as the

dx.doi.org/10.1021/ma2018827 |*Macromolecules* 2011, 44, 9164–9172

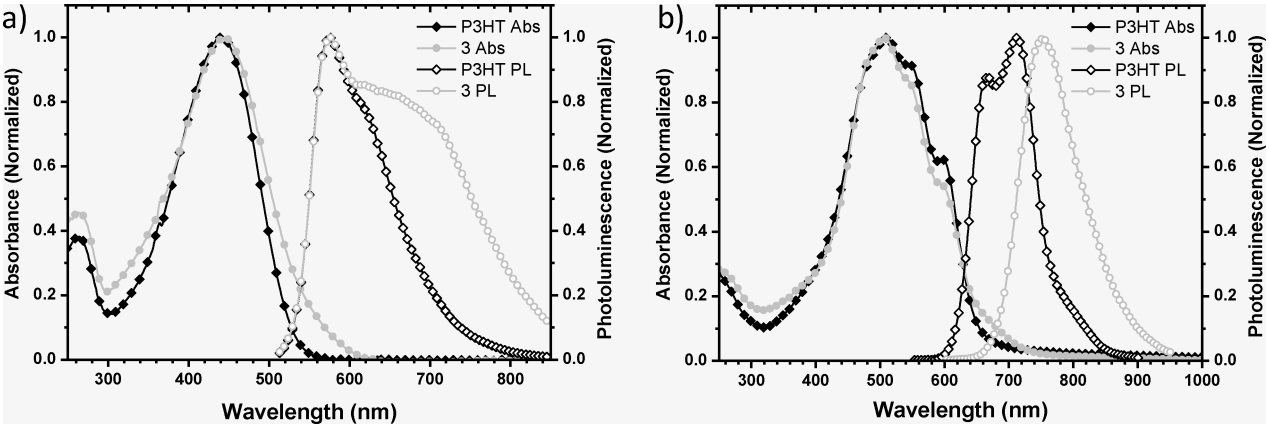

Figure 4. Steady-state UV/vis (filled symbols) and photoluminescence (open symbols) of F8TBT−P3HT **3** (gray) and a low molecular weight control P3HT sample (black) with a similar DP of 20. (a) Solution spectra and (b) thin films after heating into the melt at 200 °C for 10 min and cooling to room temperature at 10 K/min.

main product for early conversion or low molecular weights. With increasing polymerization or conversion, side reactions become prevalent and result in significant amounts of conventionally initiated P3HT. This conventional initiation is caused by the reductive coupling of F8TBT-Ni-dppe-Br, which leads to the dimer **4** and $NidppeBr_2$. Finally, an unusually high degree of termination of F8TBT-P3HT-NidppeBr takes place, leading to F8TBT-P3HT-Br, from the very beginning and continues throughout the polymerization. Scheme 2 depicts these three main mechanistic observations.

Optical Properties of F8TBT-P3HT. The optical properties of F8TBT-P3HT **3** were investigated and compared with pristine P3HT. For that purpose, steady state UV/vis and photoluminescence were measured in solution and thin film (Figure 4). The spectra of **3** were compared with a P3HT sample having 20 repeat units and a PDI of 1.13. The very similar chain length and polydispersity of **3** and the P3HT control sample are important since absorption of P3HT can strongly vary within this range of molecular weights.[42] The conjugation of the benzothiadiazole unit with the P3HT chain results in a charge transfer (CT) state, which causes a red-shifted tailing of the absorption spectra of **3** when compared to the pristine P3HT sample. This is clearly observed both in solution (Figure 4a) and in thin film (Figure 4b). It is interesting to note that the vibronic progressions in the solid state absorption of **3** are of similar intensity to the pristine P3HT sample, indicating that the amorphous F8TBT chain end does not greatly interfere with $\pi-\pi$ stacking. Differential scanning calorimetry measurements of **3** and the control P3HT sample confirm this by showing a similar crystallization enthalpy ΔH_c of 18.4 and 22.5 J/g, respectively (see Figure SI-8). The slightly lower melting enthalpy of **3** is in line with the slightly lower intensity of vibronic progressions compared to pristine P3HT (Figure 4b). This comparison is justified by the fact that the control sample and **3** have almost the same P3HT length and polydispersity and by the fact that both samples were heated into the melt and cooled down under the same controlled conditions. On comparing the photoluminescence (PL) spectra of **3** and the control sample, an even clearer difference is seen. In solution, the PL of **3** partly consists of the PL spectrum of pristine P3HT peaking at ~580 nm. In addition, a red-shifted broad band between 600 and 850 nm is seen, which is caused by emission from the CT state. Most strikingly, solid-state emission of **3** is completely red-shifted compared to pristine P3HT, and no residual P3HT emission is seen. This indicates that all excitations in the film migrate to the chain end where the electronic states are lower in energy. Interestingly, excitations in nonfunctionalized P3HT chains in sample **3** (23%) can also be transferred to functionalized F8TBT−P3HT chains in the solid state. This is significantly less likely in solution. A detailed spectroscopic investigation including time-resolved spectroscopy is currently underway.

Mechanism of BrTBT-Nidppe-Br Initiated KCTP. A high degree of end-functionalization is important not only for spectroscopic studies but also for the synthesis of well-defined conjugated systems in general. High molecular weights are important for the performance of OFET[43,44] and OPV[45] devices, which urges the identification of termination reactions. Since our observations here currently limit both of these important requirements, further mechanistic studies are necessary to understand and overcome them. We therefore turn our attention to the origin of the significant degree of termination of F8TBT-P3HT-Nidppe-Br. One possibility is that the interaction of the starting F8TBT moiety "traps" Ni(0) when "randomly walking"[46] on the P3HT chain. To further investigate this idea, we performed KCTP of **1** starting from the bifunctional initiator precursor 4,7-bis(5-bromo-4-hexyl-2-thienyl)-2,1,3-benzothiadiazole (Br-TBT-Br) **5** (Scheme 3). Using bifunctional initiators for the external initiation of KCTP has been demonstrated to be a particularly useful tool to determine the mechanism of polymerization via end group analysis. Tkachov and co-workers have synthesized a bifunctional phenyl-based initiator for the KCTP of **1**, in which Ni(0) only inserts into one phenyl−bromine bond of 1,4-dibromobenzene, thus leading to pure species Br-Ph-Nidppe-Br.[46] Owing to the relatively large aromatic core of **5**, we can expect that both possible products, the major product Br-TBT-Nidppe-Br **6** and the minor product Br-Nidppe-TBT-Nidppe-Br **7**, are formed during the reaction of **5** with $NiEt_2$bipy followed by ligand exchange (Scheme 3). Two pairs of doublets with very similar chemical shifts in the ^{31}P NMR spectrum of the initiator solution point to such a nonequivalent mixture of **6** and **7** (see Figure SI-6). It is important to note that one is still able to determine whether Ni(0)dppe can "ring walk" over the TBT bridge by analyzing the polymeric products. Therefore, similarly to the kinetic experiment shown in Figure 3, the mixture of initiators

dx.doi.org/10.1021/ma2018827 |*Macromolecules* 2011, 44, 9164–9172

Scheme 3. KCTP of 1 Using the Bifunctional Initiator Precursor 5[a]

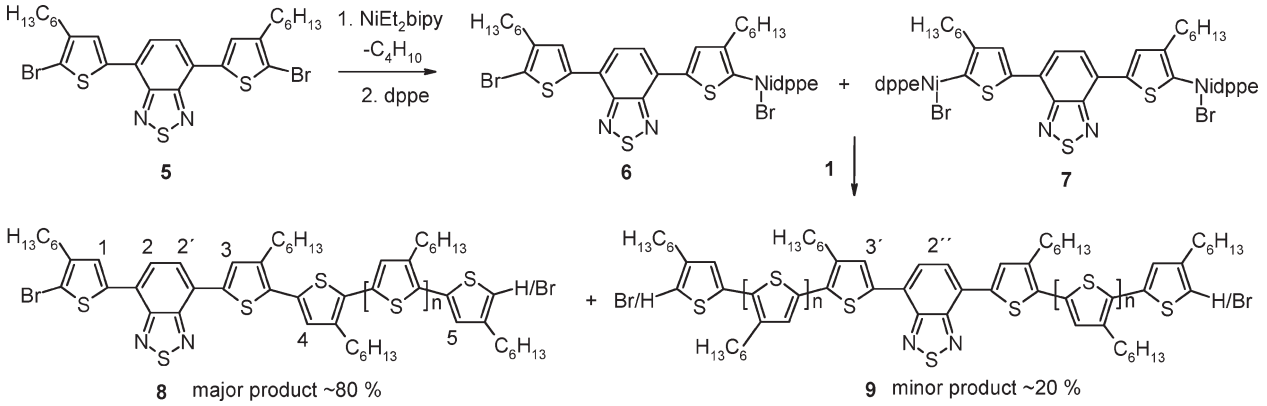

[a] The ratio of **8** and **9** depends on the initial ratio of **6** and **7** only, since Ni(0) is not able to "ring walk" over the TBT bridge.

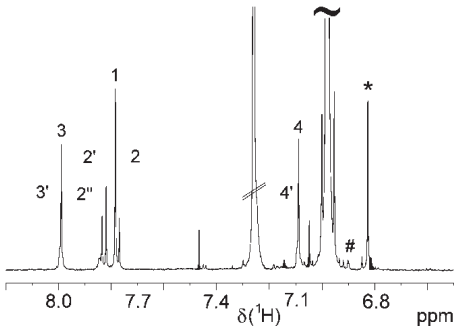

Figure 5. ^{1}H NMR spectrum (region, $CDCl_3$, 50 °C) of the polymerized product showing a 80:20 mixture of Br-TBT-P3HT (**8**; H_1−H_4, $H_{2'}$) and P3HT-TBT-P3HT (**9**; $H_{2''}$, $H_{3'}$, $H_{4'}$) (atom numbering corresponding to Scheme 3; 4 and 4′ are protons of the first thiophene unit in the growing P3HT chain after the TBT initiator; #, signal of H-terminal group; ∗, signal of Br-terminal group). The **8**/**9** ratio was determined from the integral intensities of signal regions (1 + 2) representing only **8** and (2′ + 2″) and (3 + 3′), respectively, representing **8** and **9**.

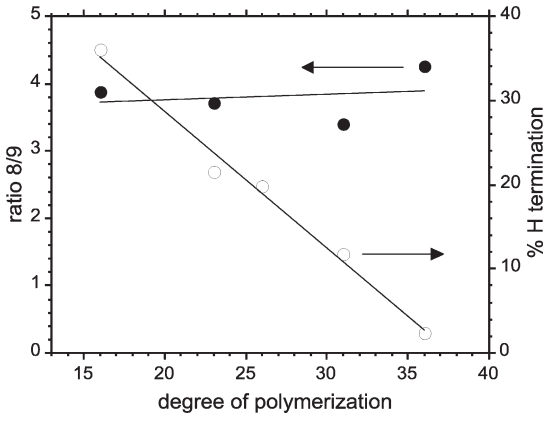

Figure 6. ^{1}H NMR end group analysis of Br-TBT-Br initiated KCTP of **1** as a function of the degree of polymerization. Solid circles: ratio **8**/**9**, open circles: fraction of living chains F8TBT-P3HT-Nidppe-Br detected as F8TBT-P3HT-H after quenching with hydrochloric acid.

6 and **7** was used to polymerize **1**. In order to demonstrate that lowering the amount of $NiEt_2$bipy with respect to the bromide precursor indeed can eliminate the reductive coupling, we used only 0.5 equiv of $NiEt_2$bipy for the in situ preparation of **6** and **7**. After ligand exchange with dppe and the addition of **1**, aliquots were withdrawn from the reaction mixture, resulting in Br-TBT-P3HT-H/Br **8** and H/Br-P3HT-TBT-P3HT-H/Br **9** and analyzed by GPC, ^{1}H NMR, and MALDI-ToF.

We are able to assign all aromatic protons in the vicinity of the TBT unit of **8** and **9** (Figure 5; for complete characterization see Figure SI-7). Using these signals, we infer a ratio of ∼4 for **8**/**9**. Interestingly, BrTBT-P3HT **8** is the major product here, which is in contrast to the results obtained from Tkachov et al., who demonstrated bidirectional growth from a phenyl-based bifunctional initiator.[46] The observation that BrTBT-P3HT **8** is the major product here gives a hint that the ability of Ni(0)dppe to "ring walk" over the TBT unit is weak if present at all, since otherwise **9** should accumulated with time and be the major product (at least for degrees of polymerizations larger than ∼24).

Polymer chains with the structure P3HT-TBT-P3HT **9** can either arise from a small percentage of Ni(0)dppe species that are able to cross the TBT bridge in **6**, thus reinitiating KCTP of **1** at the other end of the chain, or by the initially formed bifunctional initiator species **7**. To address this question, the kinetics of the polymerization were investigated by taking aliquots during the **6**/**7**-initiated KCTP of **1** and analyzed by ^{1}H NMR, GPC, and MALDI-ToF. Figure 6 shows the ratio **8**/**9** as a function of the degree of polymerization. Clearly, this ratio remains constant during polymerization, showing that Ni(0)dppe is not able to reach the other chain end to initiate polymerization there. As a result, Br-TBT-P3HT **8** cannot be converted into P3HT-TBT-P3HT **9**, which must arise from initially formed species **7**. The conversion of F8TBT-P3HT-Nidppe-Br (detected as F8TBT-P3HT-H) into F8TBT-P3HT-Br with time reveals even more details of the reaction. Figure 6 depicts how the percentage of F8TBT-P3HT-H proceeds with degree of polymerization. A rapid decrease of living chains F8TBT-P3HT-Nidppe-Br is clearly visible, and basically all chains are terminated and converted into bromine end groups after a degree of polymerization of ∼35. Since a higher monomer to initiator ratio of ∼100 was used, we conclude that practically all chains are terminated below a conversion of ∼50%.

Figure 7 shows the evolution of the MALDI spectra with time. Two peak series with varying intensity are observed for all aliquots. These correspond to Br-TBT-P3HT-H and to Br-TBT-P3HT-Br. It is important to note that chains that are grown

dx.doi.org/10.1021/ma2018827 |*Macromolecules* 2011, 44, 9164–9172

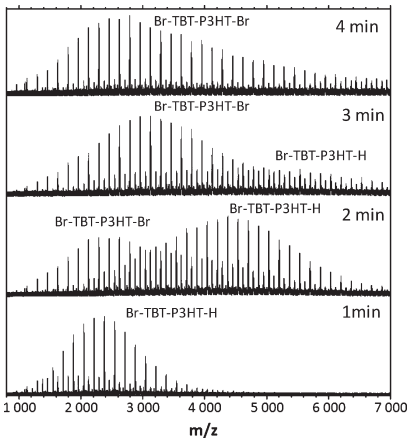

Figure 7. MALDI-ToF analysis of early aliquots during the Br-TBT-Br initiated KCTP of **1**. The major peak series in the 1 and 2 min samples corresponds to Br/H termination and thus indicate living chains, while for later polymerization times (3 and 4 min) Br/Br termination dominates.

from both sides of initiator **7**, leading to Br-P3HT-TBT-P3HT-H or Br-P3HT-TBT-P3HT-Br, and chains obtained after the polymerization from **6** are not distinguishable in MALDI-ToF. However, although both **6** and **7** are formed and initiate the KCTP of **1**, this does not result in additional peak series but it increases polydispersity. Polymers with two hydrogen end groups or any other species such as P3HT homopolymer are not observed. The rapid termination of living chains F8TBT-P3HT-Nidppe-Br into F8TBT-P3HT-Br is also clearly visible here. Only after 1 and 2 min of polymerization time do the major peak series correspond to Br-TBT-P3HT-H. In the next aliquots, almost all living chains have been terminated, leading to Br-TBT-P3HT-Br. These results are fully in line with ^{1}H NMR end group analysis and clearly show that Ni(0) is not able to "ring walk" over the TBT unit, since otherwise the conversion of Br-TBT-P3HT **8** into P3HT-TBT-P3HT **9** should lead to a nonconstant ratio **8**/**9** with time. The fraction of chains with bromine end groups approaching unity again indicates a high termination rate. Thus, molecular weight does not increase further, although conversions are below ~50% (for molecular weights and polydispersities see Figure SI-10). In principle, Ni(0)dppe can be either trapped or liberated from the chain. Since we have observed an unexpectedly stable precomplexation stage of $NiEt_2$bipy and B during initiator formation of **2e**, we suggest that the former rather than the latter phenomenon takes place here. A reductive coupling of either **6** or **7** is not observed in Figure 7, where low molecular weight dimer peaks are absent in the corresponding region. Hence, P3HT homopolymer formation did not occur either, which is evident from Figure 7 as well. This shows that the amount of $NiEt_2$bipy is an important parameter in optimizing the reaction and the extent of desired end-functionalized chains. A precise optimization of reactant equivalents remains open at this point but is important for applications where a high content of functionalized chains is required.

CONCLUSION

We have investigated the mechanism of initiator synthesis using thiophene−benzothiadiazole−thiophene (TBT) containing precursors for the Kumada catalyst transfer polycondensations (KCTP). A monofunctional and a bifunctional TBT initiator precursor were employed and successfully converted into the corresponding initiators with $NiEt_2$bipy following ligand exchange. We propose that activation of the precursor bromide occurs via precomplexation of $NiEt_2$bipy followed by reductive elimination and oxidative addition of Ni(0). After ligand exchange, the polymerization of 2-chloromagnesio-5-bromo-3-hexylthiophene (**1**) leads to the desired end-functionalized polymers; however, two main loss mechanisms are identified that can lead to side reactions and thus limit control of the reaction: Reductive coupling of the initiator occurs when a stoichiometric amount of $NiEt_2$bipy is used with respect to the precursor bromide, leading to the conventional initiation of **1** as side reaction and thus to P3HT chains that do not carry the desired functional end group. This can be avoided by lowering the equivalents of $NiEt_2$bipy, and further work should study the precise optimization of this reaction. Furthermore, the starting B units act as a trap for Ni(0) during KCTP of **1**, which results in significant chain termination, as seen by the rapid increase of bromine end groups. The external initiation of a bifunctional TBT initiator reveals that Ni(0) is not able to "ring walk" over the TBT unit. The new mechanistic processes discovered here do not currently allow for the synthesis of high molecular weight end-functionalized conjugated polymers. Therefore, only a change of the ring walking mechanism of KCTP from bidirectional[46] to unidirectional can circumvent termination reactions, thus enabling high molecular weights when grafting-from methods are to be employed. Further, we predict that more complex monomers containing TBT or benzothiadiazole alone will not readily be polymerizable under common conditions of KCTP. It will be important to understand to what extent this phenomenon is caused by specific B−Ni(0) interactions or whether it is relevant for other electron-accepting conjugated chromophores or oligomers. In order to further investigate and control interactions of Ni(0) with various such π-systems, simulations might play an important role in assisting rapid screening and complementing experimental results.

ASSOCIATED CONTENT

Supporting Information. Additional NMR experiments and complete ^{1}H NMR assignments, model reactions, differential scanning calorimetry, and GPC curves. This material is available free of charge via the Internet at http://pubs.acs.org.

AUTHOR INFORMATION

Corresponding Author
*Tel +44-1223-334319; e-mail ms928@cam.ac.uk.

ACKNOWLEDGMENT

V.S., R.T., and A.K. thank the DFG for financial support (SPP 1355 "Elementary Processes of Organic Photovoltaics", projects KI-1094/4-1 and KI-1094/3-1). M.S. and W.H. acknowledge the EPSRC for funding (Grant RG51308).

REFERENCES

(1) Arias, A. C.; MacKenzie, J. D.; McCulloch, I.; Rivnay, J.; Salleo, A. *Chem. Rev.* **2010**, *110*, 3.
(2) Sirringhaus, H. *Adv. Mater.* **2005**, *17*, 2411.
(3) Cheng, Y. J.; Yang, S. H.; Hsu, C. S. *Chem. Rev.* **2009**, *109*, 5868.
(4) Thomas, S. W.; Joly, G. D.; Swager, T. M. *Chem. Rev.* **2007**, *107*, 1339.
(5) Samuel, I. D. W.; Turnbull, G. A. *Chem. Rev.* **2007**, *107*, 1272.

(6) Grimsdale, A. C.; Chan, K. L.; Martin, R. E.; Jokisz, P. G.; Holmes, A. B. *Chem. Rev.* **2009**, *109*, 897.
(7) Miyaura, N.; Suzuki, A. *Chem. Rev.* **1995**, *95*, 2457.
(8) Carsten, B.; He, F.; Son, H. J.; Xu, T.; Yu, L. *Chem. Rev.* **2011**, *111*, 1493.
(9) Negishi, E.; Anastasia, L. *Chem. Rev.* **2003**, *103*, 1979.
(10) Wagaman, M. W.; Grubbs, R. H. *Macromolecules* **1997**, *30*, 3978.
(11) Yu, C.-Y.; Turner, M. L. *Angew. Chem.* **2006**, *45*, 7797.
(12) Yokozawa, T.; Kohno, H.; Ohta, Y.; Yokoyama, A. *Macromolecules* **2010**, *43*, 7095.
(13) Luo, K.; Kim, S. J.; Cartwright, A. N.; Rzayev, J. *Macromolecules* **2011**, *44*, 4665.
(14) Kiriy, A.; Senkovskyy, V.; Sommer, M. *Macromol. Rapid Commun.* **2011**, *32*, 1503.
(15) Iovu, M. C.; Sheina, E. E.; Gil, R. R.; McCullough, R. D. *Macromolecules* **2005**, *38*, 8649.
(16) Miyakoshi, R.; Yokoyama, A.; Yokozawa, T. *J. Am. Chem. Soc.* **2005**, *127*, 17542.
(17) Jeffries-El, M.; Sauvé, G.; McCullough, R. D. *Macromolecules* **2005**, *38*, 10346.
(18) Urien, M.; Erothu, H.; Cloutet, E.; Hiorns, R. C.; Vignau, L.; Cramail, H. *Macromolecules* **2008**, *41*, 7033.
(19) Higashihara, T.; Ohshimizu, K.; Hirao, A.; Ueda, M. *Macromolecules* **2008**, *41*, 9505.
(20) Dai, C.-A.; Yen, W.-C.; Lee, Y.-H.; Ho, C.-C.; Su, W.-F. *J. Am. Chem. Soc.* **2007**, *129*, 11036.
(21) Liu, J.; Sheina, E.; Kowalewski, T.; McCullough, R. D. *Angew. Chem.* **2002**, *41*, 329.
(22) Watanabe, N.; Mauldin, C.; Fréchet, J. M. J. *Macromolecules* **2007**, *40*, 6793.
(23) Senkovskyy, V.; Khanduyeva, N.; Komber, H.; Oertel, U.; Stamm, M.; Kuckling, D.; Kiriy, A. *J. Am. Chem. Soc.* **2007**, *129*, 6626.
(24) Smeets, A.; Van den Bergh, K.; De Winter, J.; Gerbaux, P.; Verbiest, T.; Koeckelbergh, G. *Macromolecules* **2009**, *43*, 7638.
(25) Doubina, N.; Paniagua, S. A.; Soldatova, A. V.; Jen, A. K. Y.; Marder, S. R.; Luscombe, C. K. *Macromolecules* **2011**, *44*, 512.
(26) Senkovskyy, V.; Tkachov, R.; Beryozkina, T.; Komber, H.; Oertel, U.; Horecha, M.; Bocharova, V.; Stamm, M.; Gevorgyan, S. A.; Krebs, F. C.; Kiriy, A. *J. Am. Chem. Soc.* **2009**, *131*, 16445.
(27) Khanduyeva, N.; Senkovskyy, V.; Beryozkina, T.; Horecha, M.; Stamm, M.; Uhrich, C.; Riede, M.; Leo, K.; Kiriy, A. *J. Am. Chem. Soc.* **2009**, *131*, 153.
(28) Senkovskyy, V.; Beryozkina, T.; Bocharova, V.; Tkachov, R.; Komber, H.; Lederer, A.; Stamm, M.; Severin, N.; Rabe, J. P.; Kiriy, A. *Macromol. Symp.* **2010**, *17*, 291.
(29) Kaul, E.; Senkovskyy, V.; Tkachov, R.; Bocharova, V.; Komber, H.; Stamm, M.; Kiriy, A. *Macromolecules* **2010**, *43*, 77.
(30) Senkovskyy, V.; Sommer, M.; Komber, H.; Tkachov, R.; Huck, W.; Kiriy, A. *Macromolecules* **2010**, *43*, 10157.
(31) Zaumseil, J.; McNeill, C. R.; Bird, M.; Smith, D. L.; Ruden, P. P.; Roberts, M.; McKiernan, M. J.; Friend, R. H.; Sirringhaus, H. *J. Appl. Phys.* **2008**, *103*, 064517.
(32) Svensson, M.; Zhang, F.; Veenstra, S. C.; Verhees, W. J. H.; Hummelen, J. C.; Kroon, J. M.; Inganäs, O.; Andersson, M. R. *Adv. Mater.* **2003**, *15*, 988.
(33) McNeill, C. R.; Halls, J. J. M.; Wilson, R.; Whiting, G. L.; Berkebile, S.; Ramsey, M. G.; Friend, R. H.; Greenham, N. C. *Adv. Funct. Mater.* **2008**, *18*, 2309.
(34) Hou, Q.; Zhou, Q.; Zhang, Y.; Yang, W.; Yang, R.; Cao, Y. *Macromolecules* **2004**, *37*, 6299.
(35) Miyakoshi, R.; Yokoyama, A.; Yokozawa, T. *J. Am. Chem. Soc.* **2005**, *127*, 17542.
(36) Wilke, G.; Herrmann, G. *Angew. Chem., Int. Ed.* **1966**, *5*, 581.
(37) We assume that Ni(dppe)$_2$ forms after bimolecular coupling of F8TBT-Nidppe-Br from Ni(0)dppe and a slight excess of dppe, which was used for ligand exchange.
(38) Yamamoto, T.; Abla, M. *J. Organomet. Chem.* **1997**, *535*, 209.
(39) Miyakoshi, R.; Yokoyama, A.; Yokozawa, T. *Macromol. Rapid Commun.* **2004**, *25*, 1663.
(40) Yamamoto, T.; Wakabayashi, S.; Osakada, K. *J. Organomet. Chem.* **1992**, *428*, 223.
(41) Liu, J.; Loewe, R. S.; McCullough, R. D. *Macromolecules* **1999**, *32*, 5777.
(42) Zen, A.; Pflaum, J.; Hirschmann, S.; Zhuang, W.; Jaiser, F.; Asawapirom, U.; Rabe, J. P.; Scherf, U.; Neher, D. *Adv. Funct. Mater.* **2004**, *14*, 757.
(43) Kline, R. J.; McGehee, M. D.; Kadnikova, E. N.; Liu, J.; Fréchet, J. M. J.; Toney, M. F. *Macromolecules* **2005**, *38*, 3312.
(44) Chang, J.-F.; Clark, J.; Zhao, N.; Sirringhaus, H.; Breiby, D. W.; Andreasen, J. W.; Nielsen, M. M.; Giles, M.; Heeney, M.; McCulloch, I. *Phys. Rev. B* **2006**, *74*, 115318.
(45) Schilinsky, P.; Asawapirom, U.; Scherf, U.; Biele, M.; Brabec, C. J. *Chem. Mater.* **2005**, *17*, 2175.
(46) Tkachov, R.; Senkovskyy, V.; Komber, H.; Sommer, J.-U.; Kiriy, A. *J. Am. Chem. Soc.* **2010**, *132*, 7803.